Int J Clin Exp Pathol 2014;7(11):7409-7418
www.ijcep.com /ISSN:1936-2625/IJCEP0002437

Original Article

Expression of transcription factor grainyhead-like 2 is diminished in cervical cancer

Luis A Torres-Reyes[1,2], Liliana Alvarado-Ruiz[1,2], Patricia Piña-Sánchez[3], María G Martínez-Silva[4], Moisés Ramos-Solano[1,2], Vicente Olimón-Andalón[5], Pablo C Ortiz-Lazareno[1], Georgina Hernández-Flores[1], Alejandro Bravo-Cuellar[1], Adriana Aguilar-Lemarroy[1*], Luis F Jave-Suarez[1*]

[1]División de Inmunología, Centro de Investigación Biomédica de Occidente (CIBO), Instituto Mexicano del Seguro Social (IMSS), Guadalajara, Jalisco, Mexico; [2]Programa de Doctorado en Ciencias Biomédicas, Centro Universitario de Ciencias de la Salud (CUCS)-Universidad de Guadalajara, Guadalajara, Jalisco, Mexico; [3]Laboratorio de Oncología Genómica, Unidad de Investigación Médica en Enfermedades Oncológicas, Centro Médico Nacional Siglo XXI-IMSS, Mexico; [4]Servicio de Patología, Centro Médico Nacional de Occidente-IMSS, Guadalajara, Jalisco, Mexico; [5]Escuela de Biología, Universidad Autónoma de Sinaloa. Culiacán, Sinaloa, Mexico. [*]Equal contributors.

Received September 10, 2014; Accepted October 31, 2014; Epub October 15, 2014; Published November 1, 2014

Abstract: The transcription factor grainyhead-like 2 (GRHL2) is evolutionarily conserved in many different species, and is involved in morphogenesis, epithelial differentiation, and the control of the epithelial-mesenchymal transition. It has also recently been implicated in carcinogenesis, but its role in this remains controversial. Expression of *GRHL2* has not previously been reported in cervical cancer, so the present study aimed to characterize *GRHL2* expression in cervical cancer-derived cell lines (CCCLs) and cervical tissues with different grades of lesions. Microarray analysis found that the expression of 58 genes was down-regulated in CCCLs compared to HaCaT cells (non-tumorigenic human epithelial cell line). The expression of eight of these genes was validated by quantitative real-time PCR (qPCR), and *GRHL2* was found to be the most down-regulated. Western blot assays corroborated that *GRHL2* protein levels were strongly down-regulated in CCCLs. Cervical cells from women without cervical lesions were shown to express *GRHL2*, while immunohistochemistry found that positivity to GRHL2 decreased in cervical cancer tissues. In conclusion, a loss or strong reduction in GRHL2 expression appears to be a characteristic of cervical cancer, suggesting that *GRHL2* down-regulation is a necessary step during cervical carcinogenesis. However, further studies are needed to delineate the role of GRHL2 in cervical cancer and during malignant progression.

Keywords: GRHL2, grainyhead-like 2, cervical cancer, epithelial-mesenchymal transition, carcinogenesis

Introduction

Cervical cancer is both one of the most common cancers and one of the principal causes of mortality in women worldwide (http://globocan.iarc.fr). Its main etiological factor is human papillomavirus infection [1]. Following the initial viral infection of proliferating cells in the basal layer of the cervical epithelium, infected cells proliferate and expand laterally. Viral gene expression is very tightly regulated [2], with the expression of capsid genes being activated as epithelial cells begin to mature and emigrate to suprabasal layers. The papillomavirus life cycle is time- and differentiation-dependent of the epithelial host cell, although the cellular factors involved in these processes remain unknown [3, 4].

In this context, grainyhead-like 2 (GRHL2), a member of the grainyhead subfamily of transcription factors, plays an important role in regulating epithelial cell differentiation [5-7] and has recently been implicated in carcinogenesis [8, 9]. Moreover, *GHRL2* has been suggested to control the epithelial-mesenchymal transition (EMT), with loss of the epithelial phenotype appearing to be an essential characteristic of tumor progression [10-12]. Little is known about the expression of *GRHL2* in cancer, although it was reported to be significantly down-regulated at the messenger (m)RNA and protein level in gastric cancer [8], and higher expression of *GRHL2* was observed in oral squamous cell carcinoma [13] and hepatocellular carcinoma [9]. Interestingly, dual roles of

this transcription factor were reported in breast cancer [14]. Thus, the role of *GRHL2* is still controversial, with evidence for it being both a tumor suppressor gene [8, 11, 12] and an oncogene [9, 13-17].

To the best of our knowledge there are no published reports of GRHL2 expression in cervical cancer. Therefore, in view of the important and controversial evidence previously reported from different epithelial cancers, we set out to characterize the expression of GRHL2 in cervical cancer in the present study.

Materials and methods

Cell culture

Cervical cancer-derived cell lines HeLa, SiHa, and C-33A, and the non-tumorigenic human epithelial cell line HaCaT were obtained from the German Cancer Research Center (DKFZ, Heidelberg, Germany). Cells were cultured in Dulbecco's modified Eagle's medium (DMEM) supplemented with 10% fetal bovine serum, penicillin (100 U/ml), and streptomycin (100 µg/ml), at 37°C with an atmosphere of 5% CO_2 and 90% relative humidity. All products mentioned before were acquired from GIBCO®, Life Technologies Corporation, Carlsbad, California.

RNA extraction

A total of 3-5 × 10^6 cells of each cell line were seeded on p100 culture dishes, cultured in DMEM for 24 h at 37°C, then washed with cold phosphate buffered saline. RNA extraction was performed using the RNA Mini Kit PureLinkTM (Ambion®, Life Technologies Corporation) according to the manufacturer's instructions. RNA samples were stored at -80°C until use.

Microarrays

RNA from CCCLs was analyzed by expression microarrays using the Gene Atlas Personal Microarray System (Affymetrix, Santa Clara, California). Briefly, total RNA was isolated from freshly seeded cells after 24 h of culture. The RNA integrity was assayed using the 2100 Bionalyzer (Agilent, Santa Clara, California) and 250 ng RNA from each sample was converted into double-stranded complementary (c)DNA using the WT Expression Kit (Ambion®, Life Technologies Corporation). This was then used to generate multiple copies of biotinylated cRNA by *in vitro* transcription with the GeneChip® WT Terminal Labeling and Controls Kit (Affymetrix). Biotinylated cRNA (10 µg) of each sample was hybridized to the Human Gene 1.1 ST Array Strip (Affymetrix) for 16 h at 43°C in the GeneAtlas Hybridization Station. After hybridization, microarray strips were washed and stained in the GeneAtlas Fluidics Station. Stained microarrays were scanned with the Imaging Station of the GeneAtlas System and image analysis and probe data extraction were carried out using Affymetrix GeneAtlas Software. The probe level data were summarized and normalized into probeset level data using the RMA algorithm before statistical testing; these calculations were performed using the Affymetrix expression console v. 1.1 (Affymetrix). Normalized data were analyzed using geWorkbench 2.4 software [18], and CCCL data were compared with that of HaCaT cells.

QPCR

Total RNA was reverse-transcribed into single-stranded cDNA using the SuperScript™ III First-Strand Synthesis System primed with oligo(dT) (Invitrogen™, Life Technologies Corporation). Gene expression levels were performed with 2.0 LightCycler technology using the LightCycler FastStar DNA Master PLUS SYBR Green I kit (Roche Applied Science, Penzberg, Germany). Analysis of gene expression was performed with LightCycler 4.1 software. The reference genes *ACTB*, *GADPH*, and *RPL32* were used to determine the relative quantification of target genes by the ΔΔCp method. To analyze ΔΔCp, at least two independent experiments with duplicates were conducted. These data were normalized independently with the three reference genes and analyzed relative to HaCaT cells (set as 1). Relative expression was also calculated as ΔCp by subtracting the target gene Cp minus the reference gene Cp from the same sample. This type of analysis is normally used to avoid external calibrators and to take only intrinsic references from each sample into account. Notably, ΔCp is inversely proportional to the expression of the target gene.

Western blotting

Cells were lysed with radioimmunoprecipitation assay (RIPA) buffer by sonication (15 pulses, 90% amp). Total extracts were incubated for 30 min at 4°C and subsequently centrifuged at 17,000 g for 5 min at 4°C. Protein concentrations were determined using the Bio-Rad DC Protein kit (Bio-Rad Laboratories, Hercules,

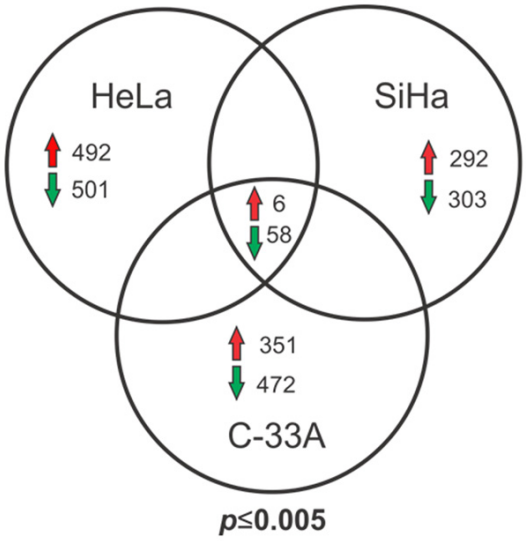

Figure 1. Venn diagram of differentially expressed genes in CCCLs versus HaCaT cells determined using microarray analysis. Comparison of genes differentially expressed between CCCLs (HeLa, SiHa, and C-33A) with respect to the keratinocyte-derived non-tumorigenic cell line HaCaT. Common up- or down-regulated genes in the three tumorigenic cell lines vs. HaCaT are shown. Statistically significant ($P \leq 0.005$).

California) and 50 µg of the extracts were electrophoresed using 8% sodium dodecyl sulfate polyacrylamide gel electrophoresis. These gels were transferred onto polyvinylidene difluoride membranes (Merck Millipore, Billerica, Massachusetts) and incubated with 5% western blocking reagent to block nonspecific binding. Primary antibodies antiRHL2 (cat. no. HPA004820, Atlas Antibodies, Stockholm, Sweden; cat. no. Ab8631, Abcam, Cambridge, United Kingdom), or anti-β-actin (cat. no. sc-1616, Santa Cruz Biotechnology, Santa Cruz, California) were incubated overnight at 4°C, and specific secondary antibodies (cat. no. sc-2005, sc-2004 and sc2020, Santa Cruz Biotechnology) were incubated for 1 h at room temperature, followed by chemiluminescent detection (cat. no. WBKLs0100, Millipore) with ChemiDoc XRS (Bio-Rad Laboratories). Densitometric analysis was carried out to determine the intensity of *GRHL2* expression relative to that of β-actin using Scion Image software (Scion Corporation, Frederick, Maryland).

Immunohistochemistry

Biopsies diagnosed as CIN 1, CIN 3 and CC were used to create tissue microarrays (TMA) by punching representative tissues for each sample with a needle to obtain 1 mm tissue cores, fixing in formalin, and transferring to a recipient paraffin block using a Tissue Microarray ATA 100 Chemicon (Temecula, California). TMA sections of 4 µm were sectioned using a Leica RM 2125 microtome (Wetzlar, Germany) and transferred to positively charged slides (Biocare Medical, Concord, California) [19]. Inmunodetection was performed automatically using the Ventana BenchMark System (Ventana Medical Systems, Mannheim, Germany) with an anti-GRHL2 antibody (cat. no. HPA004820, Atlas Antibodies) and Ultraview Universal DAB detection kit (cat. no. 760-500, Ventana Medical Systems). GRHL2 expression was evaluated by a pathologist and classified according to the level of positivity as negative, low, medium, or high.

Statistical analysis

All experiments were performed in duplicate and repeated independently at least twice. The results are expressed as means±SD. For differences between groups, analysis was performed using an unpaired, two tailed Student's *t*-test and significance at $P < 0.05$.

Results

Genes were differentially expressed between non-tumorigenic HaCaT cells and cervical cancer-derived cell lines

To identify genes with possible functions in the initiation, development, or maintenance of cervical cancer, we extracted mRNA from three CCCLs, HeLa, SiHa, and C-33A, and the keratinocyte non-tumorigenic cell line HaCaT as a control. We then compared the expression levels of comon genes using microrray analysis and identified six that were up-regulated and 58 that were down-regulated in the tumorigenic cell lines (**Figure 1**). The complete lists of differentially regulated genes are shown in Supplemental Data.

Validation of selected down-regulated genes in CCCLs by quantitative real-time qPCR

Based on the results obtained by microarray analysis, we selected eight of the 58 genes found to be down-regulated and analyzed their expression by qPCR, taking into account any relationship with neoplastic processes (**Figure 2A**). qPCR validated the down-regulation of the

A

Gene Accession	Official symbol	Official full name	Fold change (±SD)
NM_024915	GRHL2	Grainyhead-like 2	-4.62 (0.02)
NM_198173, NM_001195010, NM_021180	GRHL3	Grainyhead-like 3	-2.64 (0.06)
ENST00000338513, NM_005268	GJB5	Gap junction protein, beta 5, 31.1kDa	-4.05 (0.08)
NM_052891	PGLYRP3	Peptidoglycan recognition protein 3	-3.67 (0.04)
NM_001122965	RPTN	Repetin	-5.60 (0.03)
NM_003125	SPRR1B	Small proline-rich protein 1B	-5.75 (0.07)
NM_005988	SPRR2A	Small proline-rich protein 2A	-5.23 (0.01)
NM_001024209	SPRR2E	Small proline-rich protein 2E	-4.35 (0.03)

B

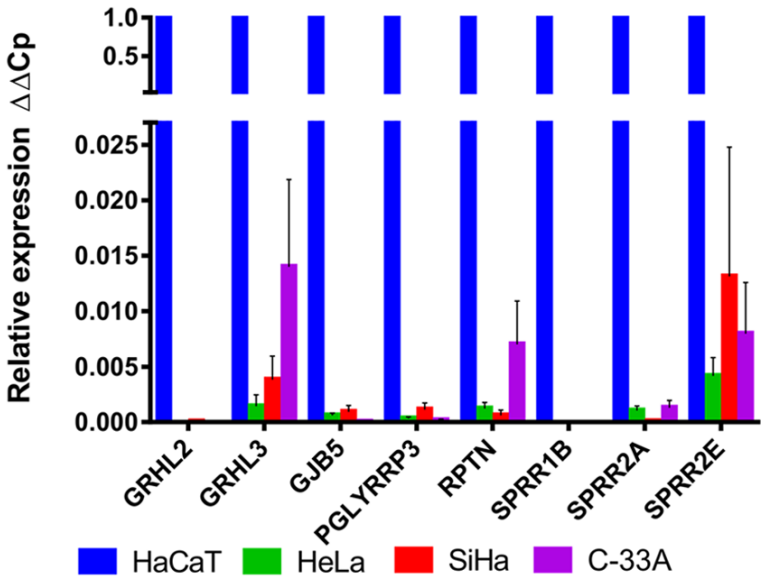

Figure 2. Down-regulated genes in CCCLs vs. HaCaT cells. A. Group of selected genes from microarray expression assays. The fold change value shown is a mean of the three CCCLs, HeLa, SiHa, and C-33A; B. Individual relative expression (ΔΔCp) of each selected gene as determined by qPCR in HeLa, SiHa, and C-33A. The values obtained were normalized to three reference genes, *ACTB*, *GAPDH*, and *RPL32*, and determined relative to HaCaT cells (set as 1). Means ± SD from at least three independent experiments are shown.

eight selected genes in CCCLs compared with HaCaT cells (**Figure 2B**). Using three different reference genes (*ACTB*, *GAPDH*, and *RPL32*) for normalization and HaCaT cells for calibration (value set as 1), relative expression values ranged from 0.015-0.000002, with *GRHL2* found to be the most down-regulated gene in CCCLs.

GRHL2 expression is remarkably decreased at the mRNA and protein level in CCCLs

In the CCCLs analyzed, two members of the Grainyhead-like family of genes (*GRHL2* and *GRHL3)* were found to be down-regulated, particularly *GRHL2*. Because the functions of these genes are closely interrelated and involved in mammalian organogenesis [20, 21] and because *GRHL2* has recently been shown to play a role in gastric and breast carcinogenesis [8, 14], we focused further on its analysis. We observed a notable difference in *GRHL2* expression (> 10 cycles) between the CCCLs and HaCaT cells when comparing amplification curves (**Figure 3A**). This difference was not observed for the reference genes, e.g. *ACTB* (**Figure 3B**).

To confirm specific amplification of primer pairs, the expected molecular weights of all qPCR products were observed on agarose gels. The relative expression of *GRHL2* in each CCCL was determined using the ΔΔCp method, and data are shown in **Figure 3C** and **3D**. These results indicated that *GRHL2* was expressed at negligible levels in CCCLs compared with HaCaT cells.

To corroborate *GRHL2* mRNA levels, protein expression was also determined. Western blotting with two different anti-GRHL2 antibodies showed that a protein of expected molecular weight was expressed only in HaCaT cells (**Figure 4A**, **4B**). Densitometric analysis revealed a 6-fold increase in GRHL2 expression in HaCaT versus HeLa, SiHa, and C-33A cells, particularly using the Atlas antibody (**Figure 4**, right panels).

GRHL2 is expressed in cervical samples without lesions

Although HaCaT cells are non-tumorigenic, they are an immortal cell line so have genomic instabilities. Therefore, to better characterize normal expression levels of *GRHL2* in keratino-

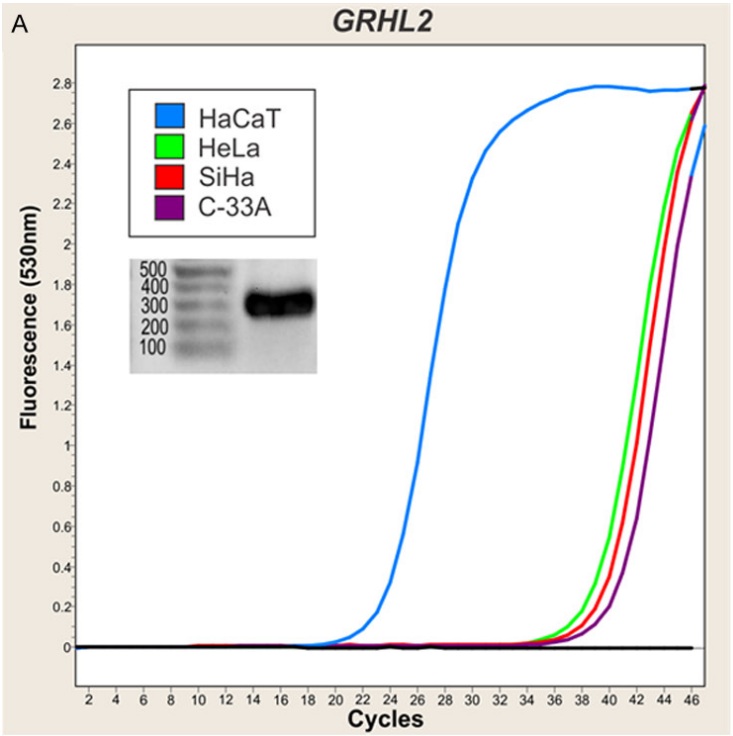

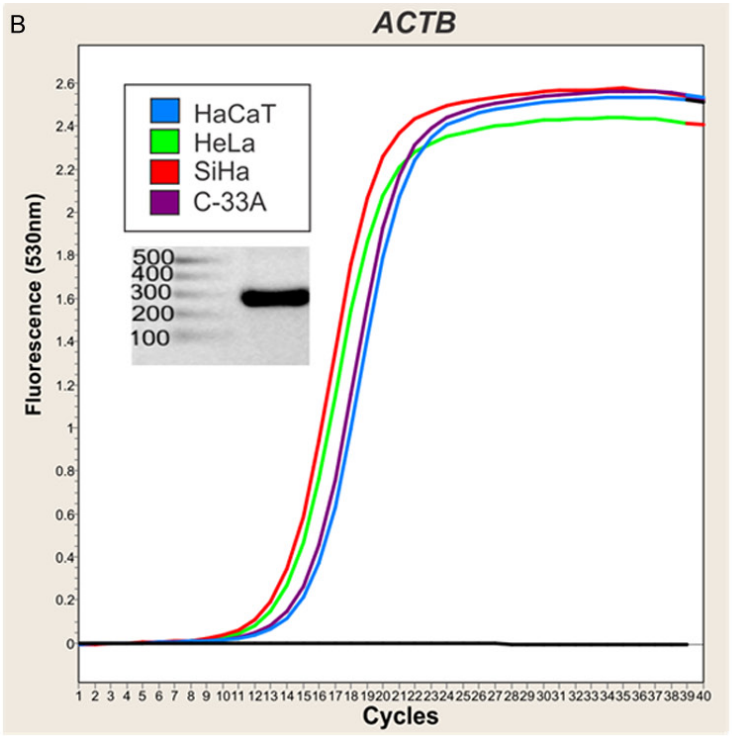

C

GRHL2 ΔΔCp				
Reference gene	HaCaT	HeLa	SiHa	C-33A
ACTB	1.00E+00	3.74E-06	7.58E-05	2.81E-06
GAPDH	1.00E+00	1.77E-06	2.82E-05	1.88E-06
RPL32	1.00E+00	2.76E-06	8.81E-05	7.95E-07
Mean	1.00E+00	2.76E-06	6.40E-05	1.83E-06
Std	0.00E+00	9.84E-07	3.16E-05	1.01E-06

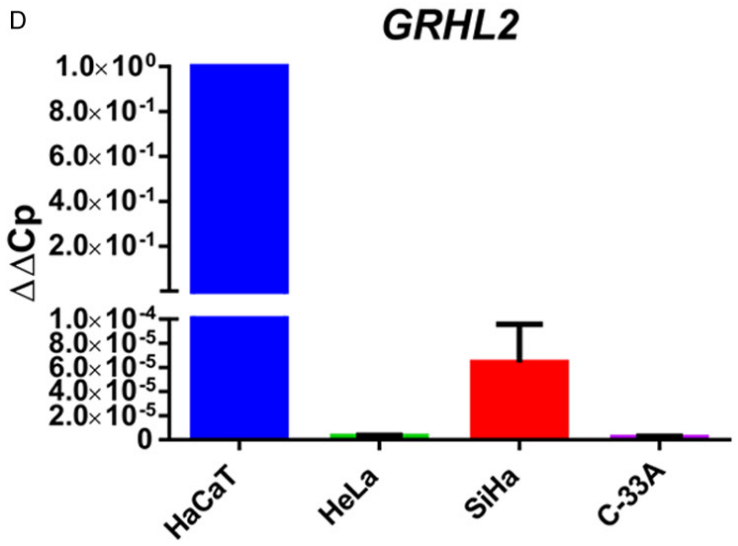

Figure 3. *GRHL2* expression as determined by qPCR. Amplification curves obtained from *GRHL2* (A) and the reference gene *ACTB* (B) in HaCaT (blue), HeLa (green), SiHa (red), and C-33A (purple). PCR products visualized on agarose gels are also shown. *GRHL2* relative expression is shown as ΔΔCp, and the values presented were normalized to each reference gene (*ACTB*, *GAPDH* and *RPL32*) and determined relative to HaCaT (C). The mean ± SD of all cell lines are displayed in a graph (D).

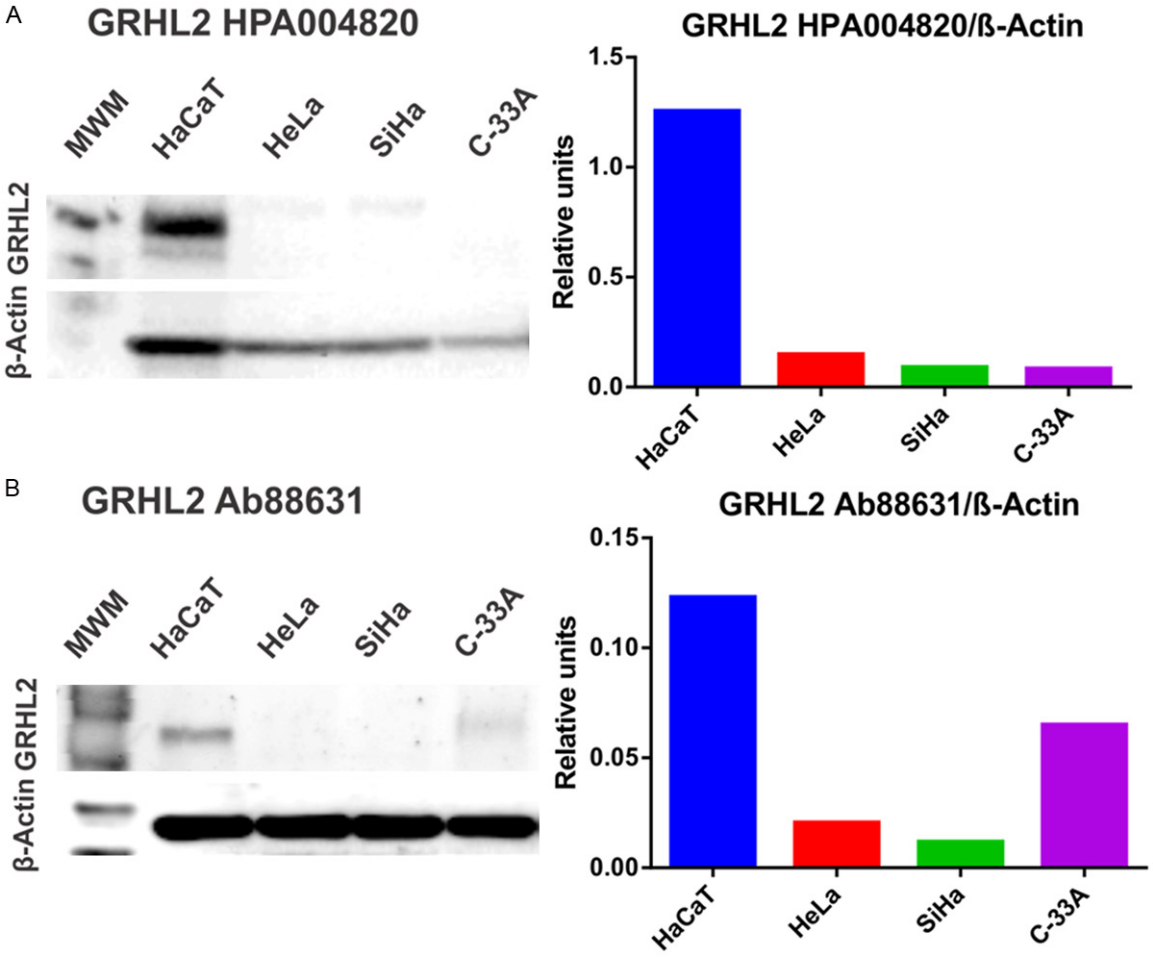

Figure 4. Detection of *GRHL2* protein expression in HaCaT, HeLa, SiHa, and C-33A using western blotting. *GRHL2* expression was measured using two independent antibodies, HPA004820-Atlas antibodies (A, left) and Ab88631-Abcam (B, left). β-actin was used as a protein loading control. Densitometric analysis expressing the ratio *GRHL2*/β-actin is also shown (A and B, right panels). MWM: Molecular weight marker.

cytes, we next determined *GRHL2* mRNA expression levels in cervical epithelial samples obtained by cervical cytobrush of women without cervical lesions (as visualized by colposcopy).

A total of 15 control cervical samples were collected for RNA extraction and retrotranscription to measure *GRHL2* expression using qPCR. ΔCp was then calculated using *ACTB*, *GAPDH*, and *RPL32* as references genes. As shown in **Figure 5**, the average ΔCp for HaCaT cells was 9.2±0.8, which was very similar to that for cervical control samples (9.1±2.7), and much lower than that for CCCLs (21.1±5.3), representing a difference of at least 10 cycles. To achieve a general perspective of *GRHL2* expression in cervical samples vs. HaCaT cells and CCCLs, ΔCps obtained from independent assays are displayed on a box and whisker plot (**Figure 5**). Cervical control samples were found to express very similar levels of *GRHL2* to HaCaT cells, whereas CCCLs showed a strongly diminished expression pattern ($P < 0.001$).

Decreased expression of GRHL2 in cervical cancer tissues

To corroborate the low expression level of *GRHL2* observed in CCCLs, tissues diagnosed

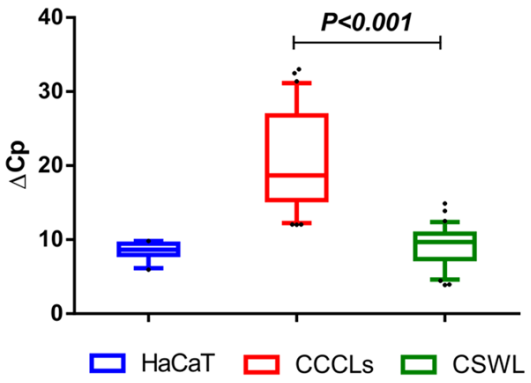

Figure 5. *GRHL2* expression at the mRNA level in cervical samples without lesions. Box plot showing relative expression levels of *GRHL2* as measured by qPCR in 15 cervical samples obtained from women without cervical lesions (CSWL). Relative expression is shown as ΔCp values (Cp of *GRHL2* minus Cp of reference gene from each sample). *ACTB*, *GAPDH*, and *RPL32* were used as reference genes. ΔCp values from HaCaT and CCCLs from all experiments are also included for comparison. The graph shows medians (dark lines), 5-95 percentile limits (boxes), interquartile ranges (whiskers), and outliers (points). *Student's *t*-test, two-tailed *P*-value < 0.001.

as cervical intraepithelial neoplasia grade 1 (CIN 1), cervical intraepithelial neoplasia grade 3 (CIN 3), as well as cervical cancer (CC), were assembled in tissue arrays to detect *GRHL2* using immunohistochemistry.

The *GRHL2* signal was evaluated by a pathologist, and representative images of the assays performed in CC and precursor lesions (CIN 1 and CIN 3) are displayed in **Figure 6A**. A summary of the results is shown in **Figure 6B**, and it was clear that *GRHL2* expression in cervical tissue samples diminished with increasing malignancy. This result is consistent with the strongly diminished GRHL2 expression observed in CCCLs (**Figure 4**).

Discussion

We used microarray expression analysis to reveal the differential expression of genes in the three CCCLs tested compared to HaCaT cells, of which *GRHL2* was strongly down-regulated in the tumorigenic cell lines (**Figure 2**). The functions of *GRHL2* are mainly related to epithelial behavior such as morphogenesis, cell polarity, differentiation, and wound healing [5-7, 22-25]. Although diminished expression of *GRHL2* has been reported in other malignant cells including human gastric carcinoma cell lines [8] and breast cancer-derived cell lines, to our knowledge no previous reports have investigated *GRHL2* expression in cervical cancer. Our study is therefore the first to demonstrate, both at the mRNA and protein level, that *GRHL2* is strongly down-regulated in CCCLs.

Previous studies of breast cancer cells with an epithelial phenotype revealed that they expressed higher levels of *GRHL2* [14, 26]. In this respect, the functional role of GRHL2 as a proto-oncogene or tumor suppressor gene remains controversial in breast carcinogenesis [10-12, 14, 15]. Additionally, the regulatory system that governs the expression of this transcription factor (*GRHL2*/ZEB1/miR-200) is not fully understood.

Similar levels of *GRHL2* as observed by qPCR in HaCaT cells were also seen in normal epithelial cervical cells (**Figure 5**), indicating that the cell line model used in our study did not misrepresent the tissue-specific level of *GRHL2* in healthy human cervical samples. This result is in agreement with previous reports of different epithelial cells such as those of the mucociliary airway epithelium and lung epithelial cells, where GRHL2 regulates processes related to morphogenesis, differentiation, and barrier functions through its transcriptional up-regulation of genes related to tight and adherent junctions [6, 7, 24, 25].

Immunohistochemistry showed that GRHL2 expression diminished in cervical tissues in line with an increase in malignancy (**Figure 6**). This supports the findings of Xiang and co-workers [8], who reported weaker GRHL2 expression in gastric cancer versus normal tissue. Similarly, Werner et al. [14] observed reduced GRHL2 expression at the invasive front of primary breast tumors, while decreased GRHL2 expression levels were also reported in the claudin-low molecular subclass of breast tumors and clear cell renal carcinomas [11]. Reduced expression of GRHL2 in breast tumors has been associated with an EMT phenotype, increased cell survival, and migratory and invasive behaviour, which is reminiscent of a tumor suppressor gene [11, 12]. Conversely, high GRHL2 expression has been related to a poor prognosis for breast cancer metastasis [10, 11, 15, 17], although we are currently exploring the hypothesis that high expression of GRHL2 indicates a loss of function of this protein.

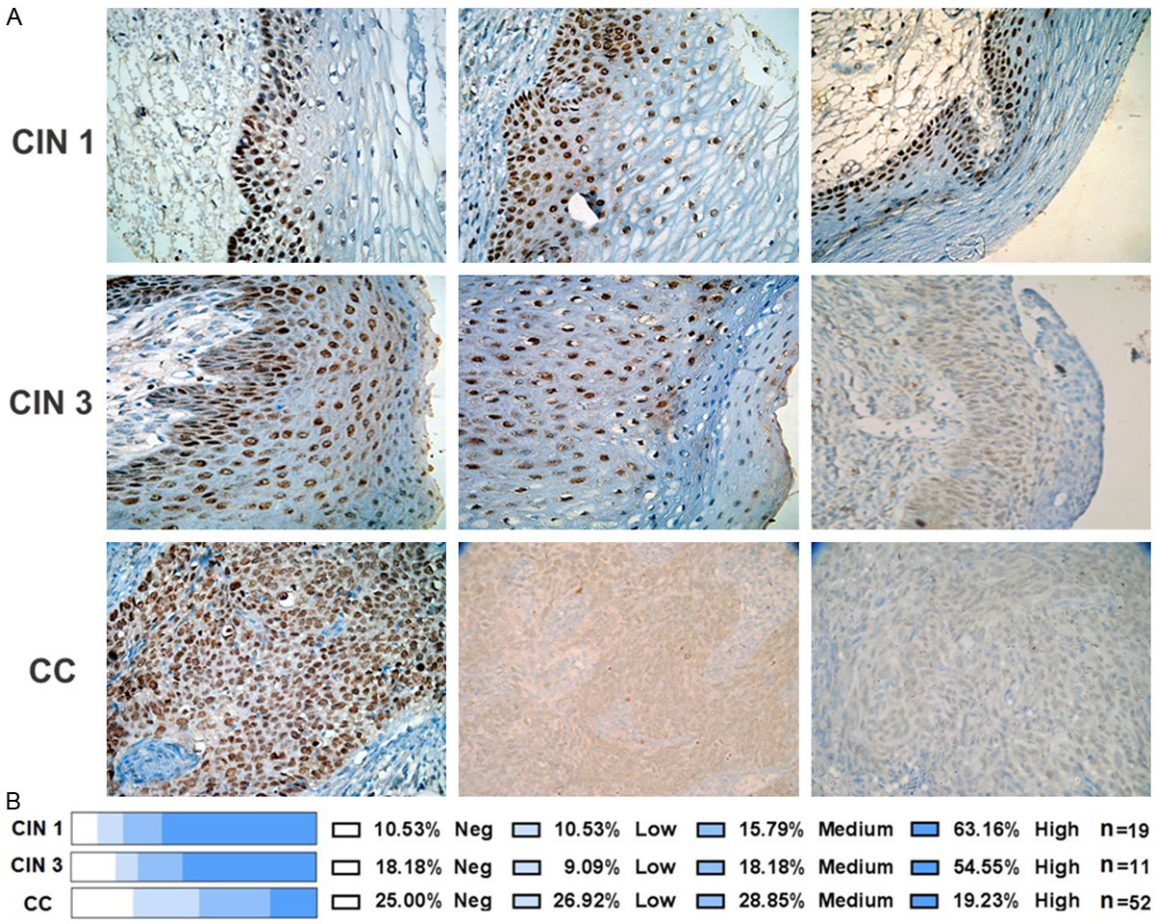

Figure 6. Immunodetection of *GRHL2* in precursor and cervical cancer tissues. Cervical tissues microarrays (including CIN 1, CIN 3, and CC biopsies) were used to detect *GRHL2* by immunohistochemistry. An anti-GRHL2 antibody (HPA004820-Atlas antibodies) was utilized as the primary antibody. Representative images from each histological diagnosis are shown at a magnification of ×40 (A). *GRHL2* expression was evaluated by the pathologist and classified according to the degree of positivity: negative, low, medium, or high. Percentages of the tissues found with the different grades of *GRHL2* positivity are included (B). The biopsies evaluated for each pathological diagnosis (*n*) are also included.

Taken together, the findings from the present study strongly indicate that loss or diminished GRHL2 expression is characteristic of cervical carcinogenesis, suggesting a tumor suppressor function for GRHL2 in this model. However, functional studies are needed to delineate its role during the malignant progression of cervical cancer cells.

Acknowledgements

LAT-R, LA-R, and MR-S are grateful for a scholarship from Consejo Nacional de Ciencia y tecnología-México. This work was supported by Fondo de Investigación en Salud-Instituto Mexicano del Seguro Social (FIS/IMSS/PROT/G12/1149).

Disclosure of conflict of interest

None.

Address correspondence to: Dr. Luis F Jave-Suarez or Dr. Adriana Aguilar-Lemarroy, División de Inmunología, Centro de Investigación Biomédica de Occidente (CIBO), Instituto Mexicano del Seguro Social (IMSS), Sierra Mojada No. 800, Col. Independencia, Guadalajara 44340, Jalisco, Mexico. Tel: +52 36170060 Ext. 31926; E-mail: lfjave@yahoo.com (LFJS); adry.aguilar.lemarroy@gmail.com (AAL)

References

[1] Psyrri A and DiMaio D. Human papillomavirus in cervical and head-and-neck cancer. Nat Clin Pract Oncol 2008; 5: 24-31.

[2] zur Hausen H. Papillomaviruses and cancer: from basic studies to clinical application. Nat Rev Cancer 2002; 2: 342-350.
[3] Stubenrauch F and Laimins L. Human papillomavirus life cycle: active and latent phases. Semin Cancer Biol 1999; 9: 379-386.
[4] Bernard HU. Regulatory elements in the viral genome. Virology 2013; 445: 197-204.
[5] Boglev Y, Wilanowski T, Caddy J, Parekh V, Auden A, Darido C, Hislop NR, Cangkrama M, Ting SB and Jane SM. The unique and cooperative roles of the Grainy head-like transcription factors in epidermal development reflect unexpected target gene specificity. Dev Biol 2011; 349: 512-522.
[6] Werth M, Walentin K, Aue A, Schonheit J, Wuebken A, Pode-Shakked N, Vilianovitch L, Erdmann B, Dekel B, Bader M, Barasch J, Rosenbauer F, Luft FC and Schmidt-Ott KM. The transcription factor grainyhead-like 2 regulates the molecular composition of the epithelial apical junctional complex. Development 2010; 137: 3835-3845.
[7] Senga K, Mostov KE, Mitaka T, Miyajima A and Tanimizu N. Grainyhead-like 2 regulates epithelial morphogenesis by establishing functional tight junctions through the organization of a molecular network among claudin3, claudin4, and Rab25. Mol Biol Cell 2012; 23: 2845-2855.
[8] Xiang J, Fu X, Ran W, Chen X, Hang Z, Mao H and Wang Z. Expression and role of grainyhead-like 2 in gastric cancer. Med Oncol 2013; 30: 714.
[9] Tanaka Y, Kanai F, Tada M, Tateishi R, Sanada M, Nannya Y, Ohta M, Asaoka Y, Seto M, Shiina S, Yoshida H, Kawabe T, Yokosuka O, Ogawa S and Omata M. Gain of GRHL2 is associated with early recurrence of hepatocellular carcinoma. J Hepatol 2008; 49: 746-757.
[10] Xiang X, Deng Z, Zhuang X, Ju S, Mu J, Jiang H, Zhang L, Yan J, Miller D and Zhang HG. Grhl2 determines the epithelial phenotype of breast cancers and promotes tumor progression. PLoS One 2012; 7: e50781.
[11] Cieply B, Riley Pt, Pifer PM, Widmeyer J, Addison JB, Ivanov AV, Denvir J and Frisch SM. Suppression of the epithelial-mesenchymal transition by Grainyhead-like-2. Cancer Res 2012; 72: 2440-2453.
[12] Cieply B, Farris J, Denvir J, Ford HL and Frisch SM. Epithelial-mesenchymal transition and tumor suppression are controlled by a reciprocal feedback loop between ZEB1 and Grainyhead-like-2. Cancer Res 2013; 73: 6299-6309.
[13] Kang X, Chen W, Kim RH, Kang MK and Park NH. Regulation of the hTERT promoter activity by MSH2, the hnRNPs K and D, and GRHL2 in human oral squamous cell carcinoma cells. Oncogene 2009; 28: 565-574.
[14] Werner S, Frey S, Riethdorf S, Schulze C, Alawi M, Kling L, Vafaizadeh V, Sauter G, Terracciano L, Schumacher U, Pantel K and Assmann V. Dual roles of the transcription factor grainyhead-like 2 (GRHL2) in breast cancer. J Biol Chem 2013; 288: 22993-23008.
[15] Yang X, Vasudevan P, Parekh V, Penev A and Cunningham JM. Bridging cancer biology with the clinic: relative expression of a GRHL2-mediated gene-set pair predicts breast cancer metastasis. PLoS One 2013; 8: e56195.
[16] Chen W, Dong Q, Shin KH, Kim RH, Oh JE, Park NH and Kang MK. Grainyhead-like 2 enhances the human telomerase reverse transcriptase gene expression by inhibiting DNA methylation at the 5'-CpG island in normal human keratinocytes. J Biol Chem 2010; 285: 40852-40863.
[17] Dompe N, Rivers CS, Li L, Cordes S, Schwickart M, Punnoose EA, Amler L, Seshagiri S, Tang J, Modrusan Z and Davis DP. A whole-genome RNAi screen identifies an 8q22 gene cluster that inhibits death receptor-mediated apoptosis. Proc Natl Acad Sci U S A 2011; 108: E943-951.
[18] Floratos A, Smith K, Ji Z, Watkinson J and Califano A. geWorkbench: an open source platform for integrative genomics. Bioinformatics 2010; 26: 1779-1780.
[19] Hidalgo A, Pina P, Guerrero G, Lazos M and Salcedo M. A simple method for the construction of small format tissue arrays. J Clin Pathol 2003; 56: 144-146.
[20] Wilanowski T, Tuckfield A, Cerruti L, O'Connell S, Saint R, Parekh V, Tao J, Cunningham JM and Jane SM. A highly conserved novel family of mammalian developmental transcription factors related to Drosophila grainyhead. Mech Dev 2002; 114: 37-50.
[21] Ting SB, Wilanowski T, Cerruti L, Zhao LL, Cunningham JM and Jane SM. The identification and characterization of human Sister-of-Mammalian Grainyhead (SOM) expands the grainyhead-like family of developmental transcription factors. Biochem J 2003; 370: 953-962.
[22] Auden A, Caddy J, Wilanowski T, Ting SB, Cunningham JM and Jane SM. Spatial and temporal expression of the Grainyhead-like transcription factor family during murine development. Gene Expr Patterns 2006; 6: 964-970.
[23] Pyrgaki C, Liu A and Niswander L. Grainyhead-like 2 regulates neural tube closure and adhesion molecule expression during neural fold fusion. Dev Biol 2011; 353: 38-49.
[24] Gao X, Vockley CM, Pauli F, Newberry KM, Xue Y, Randell SH, Reddy TE and Hogan BL. Evidence for multiple roles for grainyheadlike 2 in the establishment and maintenance of human mucociliary airway epithelium. Proc Natl Acad Sci U S A 2013; 110: 9356-9361.

[25] Varma S, Cao Y, Tagne JB, Lakshminarayanan M, Li J, Friedman TB, Morell RJ, Warburton D, Kotton DN and Ramirez MI. The transcription factors Grainyhead-like 2 and NK2-homeobox 1 form a regulatory loop that coordinates lung epithelial cell morphogenesis and differentiation. J Biol Chem 2012; 287: 37282-37295.
[26] Neve RM, Chin K, Fridlyand J, Yeh J, Baehner FL, Fevr T, Clark L, Bayani N, Coppe JP, Tong F, Speed T, Spellman PT, DeVries S, Lapuk A, Wang NJ, Kuo WL, Stilwell JL, Pinkel D, Albertson DG, Waldman FM, McCormick F, Dickson RB, Johnson MD, Lippman M, Ethier S, Gazdar A and Gray JW. A collection of breast cancer cell lines for the study of functionally distinct cancer subtypes. Cancer Cell 2006; 10: 515-527.

Supplemental Table 1. Genes up-regulated in the three CCCLs compared with HaCaT cells

Gene Accession	Official symbol and aliases	Official full name	Fold change
NM_004282	BAG2, BAG-2; dJ417I1.2	BCL2-associated athanogene 2	2.78
			3.45
			3.68
NM_001135597	CCDC88A, APE; GIV; GRDN; HkRP1; GIRDIN; KIAA1212	coiled-coil domain containing 88A	4.86
			4.93
			4.84
NM_021221	LY6G5B, G5b; C6orf19	lymphocyte antigen 6 complex, locus G5B	0.77
			2.02
			1.35
NM_153485	NUP155, N155, KIAA0791	nucleoporin 155kDa	0.60
			0.71
			0.92
NM_018434	RNF130, GP; G1RZFP; GOLIATH	ring finger protein 130	3.08
			3.39
			2.36
NM_004844	SH3BP5, SAB	SH3-domain binding protein 5 (BTK-associated)	0.94
			1.55
			2.35

Fold change observed in SiHa (black), C-33A (blue), and HeLa (red) using the geWorkbench software with a p value < 0.005.

Supplemental Table 2. Genes down-regulated in the three CCCLs compared with HaCaT cells

Gene Accession	Official symbol and aliases	Official full name	Fold Change
NM_133447, AB075855, NM_001146157	AGAP11, FAM25A	ankyrin repeat and GTPase domain Arf GTPase activating protein 11/family with sequence similarity 25, member A	-0.805
			-0.645
			-0.635
NM_058172, NM_001145794, ENST00000449651	ANTXR2, ISH; JHF; CMG2; CMG-2	anthrax toxin receptor 2	-2.335
			-2.79
			-2.745
NM_018014, NM_022893	BCL11A; EVI9; CTIP1; ZNF856; HBFQTL5; BCL11A-L; BCL11A-S; BCL11A-XL	B-cell CLL/lymphoma 11A (zinc finger protein)	-3.43
			-3.12
			-3.275
NM_001719, ENST00000450594	BMP7, OP-1	bone morphogenetic protein 7	-2.115
			-2.045
			-3.925
NM_000067	CA2, CAII; Car2; CA-II	carbonic anhydrase II	-6.25
			-6.32
			-6.105
NM_032330	CAPNS2	calpain, small subunit 2	-4.38
			-4.56
			-4.385
NM_004360, AB025106	CDH1, UVO; CDHE; ECAD; LCAM; Arc-1; CD324	cadherin 1, type 1, E-cadherin (epithelial)	-2.5
			-5.255
			-5.13
NM_001793	CDH3; CDHP; HJMD; PCAD	cadherin 3, type 1, P-cadherin (placental)	-4.405
			-5.685
			-5.505
NM_006382, U65652	CDRT1, HREP; SM25H2; C17ORF1; C17ORF1; C17ORF1A	CMT1A duplicated region transcript 1	-1.95
			-2.55
			-1.9
NM_178842	CERS3, LASS3	ceramide synthase 3	-5.715
			-5.59
			-5.615

NM_001307	CLDN7, CLDN-7; CEPTRL2; CPETRL2; Hs.84359; claudin-1	claudin 7	-5.12
			-5.455
			-4.565
NM_001843, ENST00000360099	CNTN1, F3; GP135	contactin 1	-5.875
			-5.7
			-5.74
NM_023944, ENST00000324632	CYP4F12, F22329_1	cytochrome P450, family 4, subfamily F, polypeptide 12	-1.975
			-2.685
			-2.655
NM_080927, ENST00000326857	DCBLD2; ESDN; CLCP1	oidin, CUB and LCCL domain containing 2	-1.11
			-1.12
			-2.82
NM_001944	DSG3, PVA; CDHF6	desmoglein 3	-6.955
			-6.89
			-6.76
NM_017434	DUOX1, LNOX1; THOX1; NOXEF1	dual oxidase 1	-3.635
			-3.78
			-3.74
NM_005228	EGFR	epidermal growth factor receptor	-1.51
			-4.65
			-1.75
NM_004438, BC026327	EPHA4; SEK; HEK8; TYRO1	EPH receptor A4	-2.96
			-3.21
			-3.395
NM_032333, ENST00000372181, NR_024572	FAM213A, PAMM; C10orf58	family with sequence similarity 213, member A	-2.92
			-3.775
			-3.265
AB030073, NM_000141	FGFR2, BEK; JWS; CEK3; CFD1; ECT1; KGFR; TK14; TK25; BFR-1; CD332; K-SAM	fibroblast growth factor receptor 2	-2.415
			-2.505
			-2.335
NM_014568	GALNT5, GALNAC-T5	UDP-N-acetyl-alpha-D-galactosamine:polypeptide N-acetylgalactosaminyltransferase 5 (GalNAc-T5)	-4.255
			-4.28
			-4.21
NM_198460	GBP6, GBP4 (mouse)	guanylate binding protein family, member 6	-3.86
			-3.835
			-3.825
ENST00000338513, NM_005268	GJB5, CX31.1	gap junction protein, beta 5, 31.1kDa	-4.05
			-4.05
			-3.9
NM_000405	GM2A; SAP-3; GM2-AP	GM2 ganglioside activator	-1.1
			-1.89
			-1.77
NM_024915	GRHL2, BOM; DFNA28; TFCP2L3	grainyhead-like 2 (Drosophila)	-4.565
			-4.52
			-4.525
NM_198173, NM_001195010, NM_021180	GRHL3, SOM; TFCP2L4	grainyhead-like 3 (Drosophila)	-2.705
			-2.575
			-2.64
NM_001005340, BT007074, BC011595	GPNMB, NMB; HGFIN	glycoprotein (transmembrane) nmb	-5.36
			-5.59
			-4.935
NM_002083	GPX2, GPRP; GPx-2; GI-GPx; GPRP-2; GPx-GI; GSHPx-2; GSHPX-GI	glutathione peroxidase 2 (gastrointestinal)	-6.59
			-6.535
			-6.56
NM_001009931	HRNR, FLG3; S100A16; S100a18	hornerin	-2.11
			-2.075
			-2.085

NM_021979, ENST00000394709	HSPA2, HSP70-2; HSP70-3	heat shock 70kDa protein 2	-3.1
			-3.95
			-3.67
NM_000214	JAG1; AGS; AHD; AWS; HJ1; CD339; JAGL1	jagged 1	-4.33
			-4.575
			-2.03
NM_170736	KCNJ15, IRKK; KIR1.3; KIR4.2	potassium inwardly-rectifying channel, subfamily J, member 15	-2.95
			-3.015
			-2.95
NM_005046, NM_139277, AF411214	KLK7, hK7; SCCE; PRSS6	kallikrein-related peptidase 7	-3.855
			-3.89
			-3.895
NM_000421	KRT10, BIE; EHK; K10; KPP; BCIE; CK10	keratin 10	-7.01
			-7.19
			-6.695
NM_002275, ENST00000393976	KRT15, K15; CK15; K1C0	keratin 15	-4.375
			-5.295
			-5.385
NM_001584, NM_001145399	MPPED2, 239FB; C11orf8, FETAL BRAIN PROTEIN 239 D11S302E	metallophosphoesterase domain containing 2	-4.55
			-4.64
			-3.32
NM_006158	NEFL, NFL; NF-L; NF68; CMT1F; CMT2E	neurofilament, light polypeptideprovided	-4.1
			-4.7
			-4.565
NM_001099287	NIPAL4; ICHYN; ICHTHYIN	NIPA-like domain containing 4	-3.59
			-3.58
			-3.46
NM_052891	PGLYRP3, PGRPIA; PGRP-Ialpha	peptidoglycan recognition protein 3	-3.65
			-3.735
			-3.675
NM_001029884	PLEKHG1, ARHGEF41	pleckstrin homology domain containing, family G (with RhoGef domain) member 1	-1.945
			-1.865
			-1.93
NM_001011709, ENST00000369230	PNLIPRP3	pancreatic lipase-related protein 3	-5.235
			-5.305
			-5.29
NM_198965, NM_002820, NM_198964	PTHLH, HHM; PLP; BDE2; PTHR; PTHRP	parathyroid hormone-like hormone	-5.565
			-5.63
			-5.105
NM_020387	RAB25, CATX-8; RAB11C	RAB25, member RAS oncogene family	-5.7
			-5.565
			-5.6
NM_012294, ENST00000451559	RAPGEF5, GFR; REPAC; MR-GEF	Rap guanine nucleotide exchange factor (GEF) 5	-3.83
			-3.75
			-3.7
NM_182757	RNF144B; PIR2; IBRDC2; p53RFP; bA528A10.3	ring finger protein 144B	-1.63
			-4.025
			-2.815
NM_001122965	RPTN	repetin	-5.54
			-5.57
			-5.6
NM_144777	SCEL	sciellin	-4.165
			-4.065
			-4.03
NM_002974	SERPINB4, PI11; SCCA1; SCCA2; LEUPIN; SCCA-2	serpin peptidase inhibitor, clade B (ovalbumin), member 4	-6.285
			-6.31
			-6.215

NM_198277	SLC37A2, pp11662, G3PP	solute carrier family 37 (glycerol-3-phosphate transporter), member 2, GLYCEROL-3-PHOSPHATE PERMEASE	-4.41
			-4.775
			-4.47
NM_144682	SLFN13, SLFN10	schlafen family member 13	-2.645
			-2.66
			-2.745
NM_003087, ENST00000372013, NM_006829	SNCG, SR; BCSG1, PERSYN	synuclein, gamma (breast cancer-specific protein 1)	-1.935
			-3.5
			-3.375
NM_003125	SPRR1B, SPRR1; GADD33; CORNIFIN	small proline-rich protein 1B	-5.67
			-5.825
			-5.755
NM_005988	SPRR2A	small proline-rich protein 2A	-5.23
			-5.23
			-5.21
NM_001024209	SPRR2E	small proline-rich protein 2E	-4.35
			-4.32
			-4.38
NM_018837,	SULF2, HSULF-2	sulfatase 2	-4.305
			-4.625
			-1.435
NM_019894	TMPRSS4, CAPH2; MT-SP2; TMPRSS3	transmembrane protease, serine 4	-4.94
			-4.945
			-4.91
NM_021625, AB032427	TRPV4, VRL2; CMT2C; SPSMA; TRP12; VROAC; HMSN2C; OTRPC4; SSQTL1	transient receptor potential cation channel, subfamily V, member 4	-2.46
			-1.775
			-2.49
NM_145652, ENST00000307971	WFDC5, PRG5; WAP1; dJ211D12.5	WAP four-disulfide core domain 5	-3.245
			-3.175
			-3.26

Fold change observed in SiHa (black), C-33A (blue), and HeLa (red) using the geWorkbench software with a *P* value < 0.005.